7-23-2004

The Catalytic Role of Glutamate 151 in the Leucine Aminopeptidase from *Aeromonas proteolytica*

Krzysztof P. Bzymek
Utah State University

Richard C. Holz
Marquette University, richard.holz@marquette.edu

Published version. *Journal of Biological Chemistry*, Vol. 279, No. 30 (July 23, 2004): 31018-31025. DOI.
Richard Holz was affiliated with the Utah State University at the time of publication.

THE JOURNAL OF BIOLOGICAL CHEMISTRY
Vol. 279, No. 30, Issue of July 23, pp. 31018–31025, 2004

Printed in U.S.A.

The Catalytic Role of Glutamate 151 in the Leucine Aminopeptidase from *Aeromonas proteolytica**

Received for publication, April 12, 2004, and in revised form, May 10, 2004
Published, JBC Papers in Press, May 11, 2004, DOI 10.1074/jbc.M404035200

Krzysztof P. Bzymek and Richard C. Holz‡

From the Department of Chemistry and Biochemistry, Utah State University, Logan, Utah 84322-0300

Glutamate 151 has been proposed to act as the general acid/base during the peptide hydrolysis reaction catalyzed by the co-catalytic metallohydrolase from *Aeromonas proteolytica* (AAP). However, to date, no direct evidence has been reported for the role of Glu-151 during catalytic turnover by AAP. In order to elucidate the catalytic role of Glu-151, altered AAP enzymes have been prepared in which Glu-151 has been substituted with a glutamine, an alanine, and an aspartate. The Michaelis constant (K_m) does not change upon substitution to aspartate or glutamine, but the rate of the reaction changes drastically in the following order: glutamate (100% activity), aspartate (0.05%), glutamine (0.004%), and alanine (0%). Examination of the pH dependence of the kinetic constants k_{cat} and K_m revealed a change in the pK_a of a group that ionizes at pH 4.8 in recombinant leucine aminopeptidase (rAAP) to 4.2 for E151D-AAP. The remaining pK_a values at 5.2, 7.5, and 9.9 do not change. Proton inventory studies indicate that one proton is transferred in the rate-limiting step of the reaction at pH 10.50 for both rAAP and E151D-AAP, but at pH 6.50 two protons and general solvation effects are responsible for the observed effects in the reaction catalyzed by rAAP and E151D-AAP, respectively. Based on these data, Glu-151 is intrinsically involved in the peptide hydrolysis reaction catalyzed by AAP and can be assigned the role of a general acid and base.

Hydrolases that contain co-catalytic metallo-active sites play important roles in numerous biological processes including hormone regulation, insulin degradation, neurological function, and antibiotic resistance (1, 2). Within this group, several have been crystallographically characterized, such as the leucine aminopeptidases from *Aeromonas proteolytica* (*Vibrio proteolyticus*) (AAP),[1] *Streptomyces griseus*, and bovine lens, a number of β-lactamases, *X*-Pro aminopeptidases, insulin-degrading enzyme, as well as carboxypeptidase G_2 from *Pseudomonas* sp. strain RS-16 (2–5). Enzymes with active sites that are superimposable on AAPs, such *S. griseus* aminopeptidase, the D-aminopeptidase from *Bacillus subtilis* (DppA), the *dapE*-encoded *N*-succinyl-L,L-diaminopimelic acid desuccinylase (DapE), the *argE*-encoded *N*-acetyl-L-ornithine deacetylase (ArgE), carboxypeptidase G_2, and glutamate carboxypeptidase II, sometimes referred to as *N*-acetylated α-linked acidic dipeptidase, all play important roles in living organisms (1, 2, 6–8). For instance, because of the location of glutamate carboxypeptidase II in the central and peripheral nervous systems, it is believed to play a critical role in modulating the release of glutamate (9, 10). The role of *N*-acetylaspartylglutamate has been extensively studied, and among other functions, it serves as a negative modulator of glutamatergic neurotransmission (11–14). There is also mounting evidence that *N*-acetylaspartylglutamate is involved in neuropsychiatric disorders associated with the dysregulation of glutamatergic neurotransmission, such as schizophrenia, seizure disorders, Parkinson's disease, and amyotrophic lateral sclerosis (15). For this reason, these metallohydrolases have become the subject of intense efforts in inhibitor design (16).

AAP possesses ideal properties for the study of hydrolysis reactions catalyzed by co-catalytic metal centers (17). AAP is a small monomeric enzyme (32 kDa.) that contains two g atoms of Zn(II) per mol of polypeptide, is thermostable for several hours at 70 °C, can be obtained in large quantities (>100 mg), and can be genetically manipulated (2, 17).[2] AAP has been crystallographically characterized and possesses a (μ-aqua)(μ-carboxylato)dizinc(II) core with a terminal carboxylate and histidine residue coordinated to each metal ion (19). Both zinc ions reside in a distorted tetrahedral coordination geometry with a Zn-Zn distance of 3.5 Å. In addition, several x-ray crystal structures of inhibited forms of AAP have been reported (20–22). The native Zn(II) ions can be replaced with other metal ions in a sequential fashion, providing highly active forms of the enzyme (23). That the metal ions can be sequentially replaced to yield specific heterodimetallic forms of the enzyme has proved extremely useful in mechanistic studies involved in probing the roles of each individual metal ion (2). Whereas AAP is not a specific target for pharmaceuticals at this time, a detailed understanding of its mechanism is still quite important with regard to other metallohydrolases that contain co-catalytic active sites that are drug targets (1–3). For these reasons, AAP is one of the best mechanistically characterized hydrolytic enzymes with a co-catalytic metallo-active site (2).

Comparison of one and two metal-containing peptidases with known x-ray crystal structures reveals some common features for both mono- and dinuclear hydrolases (24–27). All have at least one bound water molecule and many contain an active site carboxylate residue that does not function as a metal ligand. This carboxylate residue, usually a glutamate, often forms a hydrogen bond to a water molecule that is also bound to an active site metal ion. The x-ray crystal structure of AAP

* This work was supported by National Science Foundation Grant CHE-0240810 (to R. C. H.). The costs of publication of this article were defrayed in part by the payment of page charges. This article must therefore be hereby marked "*advertisement*" in accordance with 18 U.S.C. Section 1734 solely to indicate this fact.

‡ To whom correspondence should be addressed: Dept. of Chemistry and Biochemistry, Utah State University, Logan, UT 84322-0300. Tel.: 435-797-2609; Fax: 435-797-3390; E-mail: rholz@cc.usu.edu.

[1] The abbreviations used are: AAP, leucine aminopeptidases from *A. proteolytica*; rAAP, recombinant leucine aminopeptidase; L-*p*NA, L-leucine-*p*-nitroanilide; MES, 2-(*N*-morpholino)ethanesulfonic acid; MOPS, 3-(*N*-morpholino)propanesulfonic acid; Tricine, (*N*-tris[hydroxymethyl]methylglycine; WT, wild type.

[2] K. P. Bzymek, V. M. D'souza, G. Chen, H. Campbell, A. Mitchell, and R. C. Holz, submitted for publication.

TABLE I
Comparison of the observed kinetic parameters for rAAP and Glu-151-AAP

	rAAP	E151Q	E151A	E151D
K_m (μm)	14.3 ± 0.4	18.8 ± 2.3		17.8 ± 0.3
Specific activity (units/mg)[a]	126 ± 1	0.005 ± 1 × 10^{-4}		0.069 ± 0.003
k_{cat} (min^{-1})	4280 ± 42	0.160 ± 0.005	ND[b]	2.24 ± 0.01

[a] The assays were performed in 10 mM Tricine buffer (pH 8.0), 0.2 M KCl, and 0.1 mM $ZnSO_4$ using L-*p*NA as the substrate.
[b] ND, none detected.

reveals that an oxygen atom of Glu-151 forms a hydrogen bond with a water molecule that bridges the two Zn(II) ions (19). Glu-151 has been proposed to act as the proton shuttle during catalytic turnover, but no direct evidence has been reported to substantiate this hypothesis (22). In order to gain insight into the catalytic role of Glu-151, we have prepared the E151D, E151Q, and E151A altered AAP enzymes and characterized each by kinetic and spectroscopic methods. These data suggest that Glu-151 functions as the general acid/base during the hydrolysis of N-terminal polypeptides by AAP.

MATERIALS AND METHODS

Protein Expression and Purification—All chemicals used in this study were purchased from commercial sources and were of the highest quality available. The plasmid encoding the 51-kDa form of AAP (pVS-NMC) (28)[2] was obtained from Prof. Kiyoshi Hayashi. Growth conditions, processing, and purification of the recombinant protein were prepared as described previously.[2]

Site-directed Mutagenesis—Altered forms of AAP were obtained by PCR mutagenesis using the following primers: 5′-TG GCT TAT GCC GCT *XXX* GAA GTC GGC TTG CGTG-3′ and 5′-CACG CAA GCC GAC TTC YYY AGC GGC ATA AGC CA-3′ with GCG, GAC, CAG for *XXX* and CGC, GTC, CTG for YYY of E151A, E151D, and E151Q mutants, respectively. Site-directed mutants were obtained using the QuickChange™ site-directed mutagenesis kit (Stratagene, La Jolla, CA) following the manufacturer's procedures. Reaction products were transformed into *Escherichia coli* XL1-Blue competent cells (*recA1 endA1 gyrA96 thi-1 hsdR17supE44 relA1 lac* [*F′ proAB lacI*^{q}*ZΔM15 Tn10 (Tet*^{r})]), grown on LB-agarose plates containing kanamycin at a concentration of 50 μg/ml. A single colony of each mutant was grown in 50 ml of LB containing 50 μg/ml kanamycin. Plasmids were isolated using Wizard Plus Minipreps DNA purification kit (Promega, Madison, WI) or Qiaprep® Spin Miniprep kit (Qiagen, Valencia, CA). Each mutation was confirmed by DNA sequencing (Utah State University Biotechnology Center). Plasmids containing the altered AAP genes were transformed into *E. coli* BL21 Star™ (DE3) (*F*$^-$ *ompT hsdS*$_B$ (*r*$_B$$^-$*m*$_B$$^-$) *gal* dcm *rne131* (DE3)) (Invitrogen) (28).[2]

Enzymatic Assay—Recombinant and Glu-151-altered forms of AAP were assayed for catalytic activity using L-leucine-*p*-nitroanilide (L-*p*NA) as the substrate (17). In this assay, the hydrolysis of L-*p*NA was measured spectrophotometrically by monitoring the formation of *p*-nitroaniline at 405 nm (ϵ = 10,800 M^{-1} cm^{-1}). All assays were performed on a Shimadzu UV-3101PC spectrophotometer equipped with a constant temperature cell holder and an Isotemp 2013D water bath (Fisher). Enzyme concentrations were determined from the absorbance at 280 nm with the value ϵ_{280} = 43,950 M^{-1} cm^{-1} (29). All assays were performed at 25 ± 0.1 °C in 10 mM Tricine buffer (pH 8.0) with 0.1 mM $ZnSO_4$, unless stated otherwise.

pH Profiles—The enzymatic activity of rAAP and the E151D form of AAP at pH values between 4.5 and 10.75 was measured using L-*p*NA as the substrate. The conditions and methods used were identical to those described by Baker and Prescott (30). Briefly, the concentration of each buffer used was 10 mM, and the following buffers were used: carbonate (pH 10.75); borate (pH 8.50–10.50); Tricine (pH 7.00–8.50); MOPS (pH 6.50–7.00); MES (pH 5.50–6.50); acetate (pH 4.50–5.50). No additional Zn(II) was included in any of the buffers listed above pH 8.50. Between pH 6.00 and 8.50, 0.1 mM Zn(II) was included in all the buffers. At pH values below 6.0, three buffers were prepared at each pH that contained different concentrations of Zn(II) (typically ranging between 0.1 and 10 mM), to ensure that Zn(II) depletion did not affect the kinetic measurements. The kinetic parameters k_{cat}, K_m, and k_{cat}/K_m were determined by using 8–12 different substrate concentrations ranging from 0.2 to 10.0 times the observed K_m value at each pH studied. Kinetic parameters and fits to the kinetic curves were obtained using Igor Pro (Wavemetrix Inc., Lake Oswego, OR) by fitting the experimental data to the appropriate equations.

Solvent Isotope Effect—All buffers were prepared from a freshly opened bottle of 99.9% [^{2}H]H_2O (Aldrich). The buffers and Zn(II) salts used in the preparation of all deuterated buffers were in the anyhydrous form. The buffer used for measurements at pH 10.50 (10 mM carbonate) did not contain any Zn(II) because Zn(II) hydroxide precipitates under these conditions. The buffer used at pH 6.50 (10 mM MES) contained 0.5 mM $ZnCl_2$ to ensure that no Zn(II) depletion would occur during the experiment. The pH of each buffer used was adjusted by the addition of NaOD or DCl (both 99%+ deuterium content; Acros Organics, Geel, Belgium) and corrected for deuteration by adding 0.4 to the reading of the pH electrode.

Apoenzyme Preparation—Purified and concentrated protein (10–20 mg/ml) was incubated with 10–15 mM disodium EDTA at 4 °C until no activity was observed (usually 1–3 days). To remove the EDTA, the protein was dialyzed extensively against 100 times the volume of metal-free (chelexed) 50 mM HEPES buffer (pH 7.5). The activity of the dialyzed protein was less than 1% of the activity of the protein reconstituted with 2 eq of Zn(II). All plasticware used for dialysis and the dialysis tubing was presoaked in a disodium EDTA/bicarbonate solution to remove all traces of metals and then extensively washed with 18 ohm nanopure water (NANOpure Ultra Pure Water System, Barnstead/Thermolyne, IA) and chelexed HEPES buffer (pH 7.5).

Spectroscopic Measurements—Electronic absorption spectra were recorded on a Shimadzu UV-3101PC spectrophotometer. All solutions used were degassed prior to the experiment. Apo-rAAP (typically 1 mM) was incubated with Co(II) ($CoCl_2$, ≥99.999% Acros Organics, Geel, Belgium) for ~10 min at 25 °C. Apoprotein absorbance was subtracted from the spectra obtained with Co(II) using Igor Pro (Wavemetrix Inc., Lake Oswego, OR).

RESULTS

Kinetic Studies on rAAP and Altered-AAP Enzymes—The K_m and k_{cat} values for rAAP, E151D-AAP, and E151Q-AAP were obtained by directly fitting the observed data to the Michaelis-Menten equation (Table I).[2] The observed k_{cat} values for E151D-AAP and E151Q-AAP were 1.9 × 10^2 and 2.7 10^4 times slower, respectively, than WT AAP (10 mM Tricine buffer (pH 8.0), 0.2 M KCl, 0.1 mM $ZnSO_4$). Most interesting, the observed K_m values for E151D-AAP and E151Q-AAP do not change significantly upon the substitution of the glutamate. When Glu-151 is replaced with a residue that cannot transfer a proton (E151A), no activity is observed.

Metal Binding Properties of E151D AAP—Electronic absorption spectra of the E151D-altered AAP enzyme were recorded in the presence of 1 and 2 eq of Co(II) ([Co_(E151D-AAP)] and [CoCo(E151D-AAP)]) (Fig. 1). The addition of 1 eq of Co(II) to E151D-AAP at pH 7.5 provides a visible absorption spectrum with a λ_{max} value of 525 nm (ϵ_{525} ~25 M^{-1} cm^{-1}). Addition of a 2nd eq of Co(II) increases the molar absorptivity at 525 nm to ~45 M^{-1} cm^{-1}. The addition of more than 2 eq of Co(II) does not alter the position of the observed absorption band but increases the molar absorptivity to ~85 M^{-1} cm^{-1} after the addition of 6 eq of Co(II) (Fig. 1).

Plots of molar absorptivity at 525 nm *versus* equivalents of Co(II) (Fig. 2) allowed the Co(II) dissociation constants for the first (K_{d1}) and second (K_{d2}) metal-binding sites to be obtained by fitting the electronic absorption titration data to Equation 1 (31),

$$r = p(K_{d1} \cdot C_S/(1 + K_{d1} \cdot C_S)) + q(K_{d2} \cdot C_S/(1 + K_{d2} \cdot C_S)) \quad \text{(Eq. 1)}$$

where p and q are the number of sites; C_S is the free metal concentration; and r is the binding function that was calculated

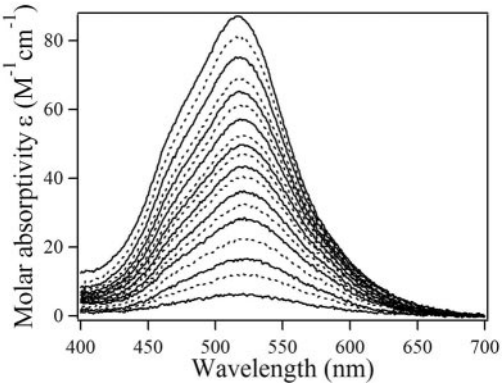

FIG. 1. **Co(II) titration of E151D AAP.** Co(II) was added in 0.25-eq increments up to 3 eq, after which 0.5-eq increments of Co(II) were added to 5 eq, and 1-eq increments were added to 8 eq of Co(II).

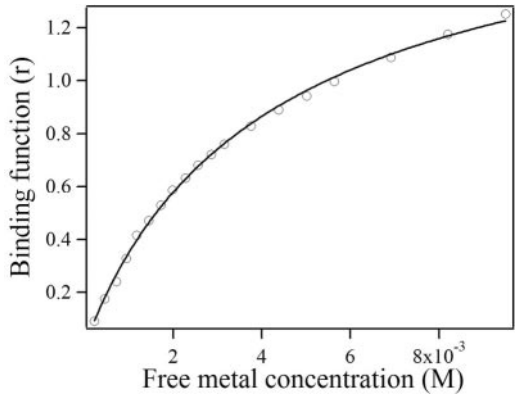

FIG. 2. **Plot of binding function, *r*, *versus* free metal concentration, C_S, for the titration of Co(II) into E151D-AAP.** The *solid line* represent the fit of the spectroscopic data (Fig. 1) to Equation 1.

by conversion of the fractional saturation ($r = f_a \times p$) as described previously (32). The free metal concentration was calculated from Equation 2,

$$C_S = C_{TS} - rC_A \qquad \text{(Eq. 2)}$$

where C_{TS} and C_A are the total molar concentrations of metal and enzyme, respectively. The best fit obtained exhibited p and q values of one and K_{d1} and K_{d2} values of 95 + 15 and 400 + 50 μM for Co(II) binding to the first and second metal-binding sites of E151D AAP, respectively.

pH Dependence of the Kinetic Parameters—In order to further characterize the role of Glu-151 in the catalytic mechanism of AAP, the kinetic parameters K_m, k_{cat}, and k_{cat}/K_m were recorded as a function of pH for both rAAP and E151D-AAP (Figs. 3 and 4). Loss of Zn(II) from AAP has been shown to occur at pH values lower than 6.0 (30), due to ionization of the metal ligands in the active site of AAP. To prevent the decrease of activity at lower pH due to Zn(II) depletion and thus erroneous analysis of pH dependence plots, at pH values of 6.0 and below data were collected at three different Zn(II) concentrations. This ensures the presence of saturating amounts of Zn(II) so the equilibrium is shifted toward the formation of Zn(II)-enzyme complex. Kinetic parameters were obtained from reciprocal plots of $1/k_{cat}$ *versus* 1/[Zn] and $1/K_m$ *versus* 1/[Zn] by extrapolation of the kinetic parameters to saturating Zn(II) concentrations, as described in detail by Baker and Prescott (30).

The rate equation used (Equation 3) was derived from a model proposed by Baker and Prescott (30) that included the ionization of two groups on the enzyme as well as the ionization of the substrate in the pH range examined.

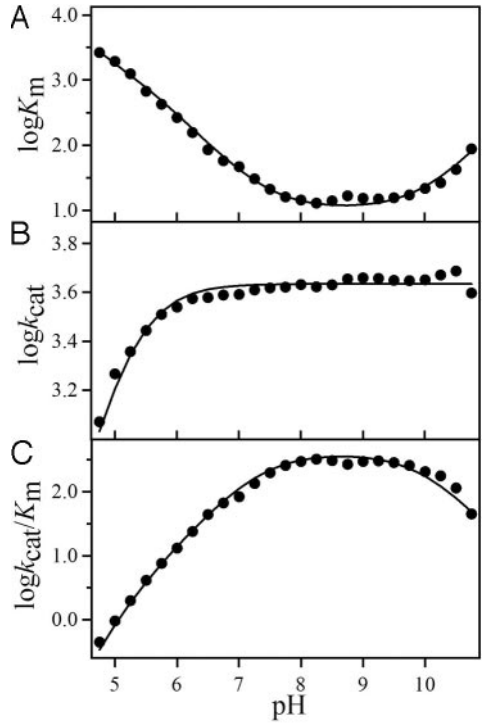

FIG. 3. **pH dependence of the kinetic parameters for the hydrolysis of L-*p*NA by rAAP.** *A*, pH dependence of K_m; *B*, pH dependence of k_{cat}; *C*, pH dependence of $\log(k_{cat}/K_m)$. The *solid lines* represent fits to Equations 2 (*A*), 3 (*B*), and 4 (*C*). All *error bars* are smaller than the symbols used.

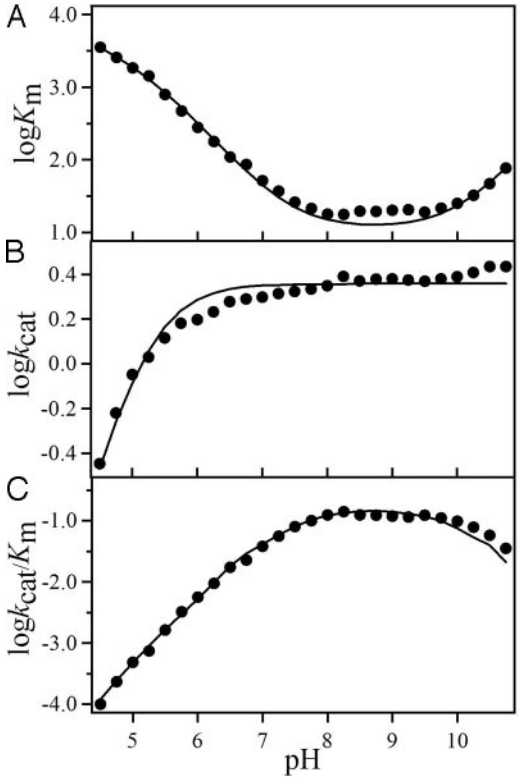

FIG. 4. **pH dependence of the observed kinetic parameters for the hydrolysis of L-*p*NA by E151D-AAP.** *A*, pH dependence of K_m; *B*, pH dependence of k_{cat}; *C*, pH dependence of $\log(k_{cat}/K_m)$. The *solid lines* represent fits to Equations 2 (*A*), 3 (*B*), and 4 (*C*). All *error bars* are smaller than the symbols used.

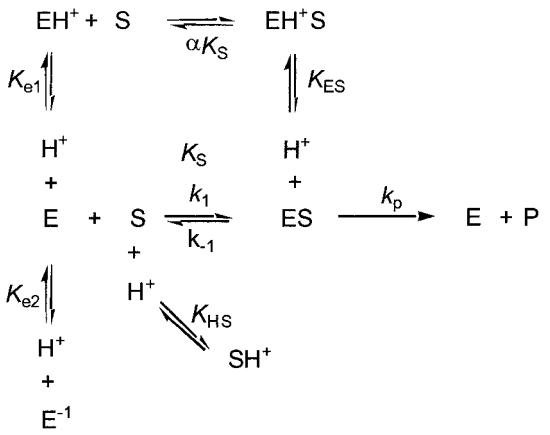

SCHEME 1

$$v = ((k_p[E]_t[S])/(1 + [H^+]/K_{HS}))/([S]_t + K_S(1 + [H^+]/K_{e1} + K_{e2}/[H^+])(1 + [H^+]/K_{HS})/(1 + [H^+]/K_{ES})) \quad \text{(Eq. 3)}$$

From Equation 3, the pH dependence of K_m and k_{cat} were obtained as shown in Equations 4 and 5:

$$K_m = K_S(1 + [H^+]/K_{e1} + K_{e2}/[H^+])(1 + [H^+]/K_{HS})/(1 + [H^+]/K_{ES}) \quad \text{(Eq. 4)}$$

$$k_{cat} = k_p/(1 + [H^+]/K_{ES}) \quad \text{(Eq. 5)}$$

Finally, k_{cat}/K_m is defined as shown in Equation 6,

$$k_{cat}/K_m = k_p/K_S(1 + [H^+]/K_{e1} + K_{e2}/[H^+])(1 + [H^+]/K_{HS}) \quad \text{(Eq. 6)}$$

Although this model is simple (Scheme 1), it is supported by a great deal of kinetic, spectroscopic, and structural data (17, 19–23, 33–43) and is consistent with the proposed mechanism of peptide hydrolysis by dinuclear metalloenzymes (2). In addition, the goodness of the fits to the kinetic data suggests that the proposed model accurately approximates the changes observed at various pH values.

Fits of the pH dependence of logK_m to Equation 4 for rAAP (Fig. 3*A*) revealed inflection points at 4.8, 5.3, 7.5, and 9.9 identical to that reported by Baker and Prescott (30) for WT AAP. For E151D-AAP, four inflection points were also observed but at 4.2, 5.0, 7.5, and 10.0 (Fig. 4*A*). Based on fits of logk_{cat}, no change in k_{cat} was observed for rAAP in the pH range 7.0–10.75, but a sharp drop in k_{cat} was observed below pH values of 6.0 with a single inflection at 5.2 (Fig. 3*B*), identical to that reported by Baker and Prescott (30) for WT AAP. Similar changes were observed for E151D-AAP and provided a pK_a value of 5.2, identical to that of rAAP (Fig. 4*B*). A plot of logk_{cat}/K_m *versus* pH for rAAP, fit to Equation 6, shows one inflection point in the acidic range at pH 5.0, one in the basic range at pH 9.9, and a free substrate ionization at pH 7.4 (Fig. 3*C*). An identical plot for E151D-AAP, revealed inflection points at pH 4.2 and pH 9.9 along the free substrate ionization at pH 7.5 (Fig. 4*C*).

Based on the proposed model, the remaining kinetic parameters, K_S and k_p, describe the substrate binding step and the rate constant of the rate-limiting step, respectively. The average value of K_S for rAAP and E151D-AAP obtained from fits to Equations 4 and 6, was 10.8 and 11.2 μM, respectively. The kinetic constant k_p, calculated using Equation 5, was 72 s^{-1} for rAAP and 0.038 s^{-1} for E151D-AAP (Table I). k_p values obtained from these fits are essentially the same as the experimentally derived k_{cat}, at pH 8.0.

Solvent Isotope Effect Studies—The solvent isotope effect for both rAAP and E151D-AAP was determined using L-*p*NA as the substrate at pH values of 6.50 and 10.50 (44). These data were plotted as atom fraction of deuterium *versus* V_n/V_D, where

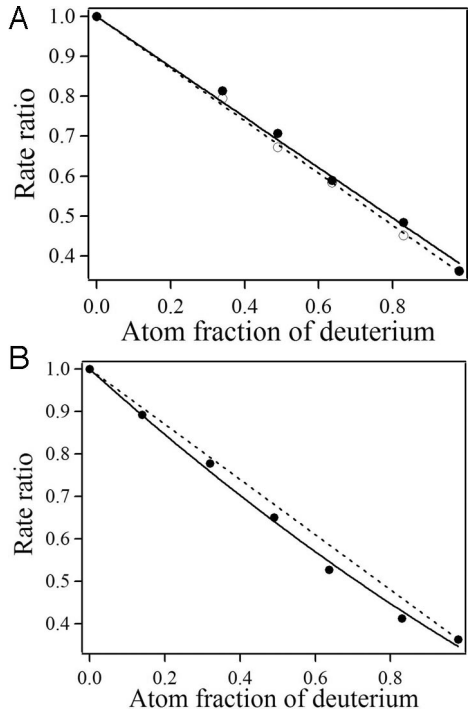

FIG. 5. **Plots of proton inventory at pH (*A*) 10.5 and (*B*) 6.5.** *A*, the *solid circles* are data obtained for rAAP (fit, *straight line*); *open circles* are experimental data obtained for E151D-AAP (fit, *dashed line*). Fractionation factors were obtained by fitting the experimental data to Equation 7. *B*, the *dashed line* represents a linear relationship, and the *solid line* is a direct fit to Equation 8 providing fractionation factors.

V_n is equal to the k_{cat} value obtained at a particular fraction of deuterium, whereas V_D is k_{cat} in buffer containing 100% deuterium oxide (Figs. 5 and 6). Proton inventories were obtained by fitting the experimental data to equations derived from the Gross-Butler Equation 7,

$$V_n/V_0 = \frac{\prod_i^{V_T}(1 - n + n_i^T)}{\prod_i^{V_R}(1 - n + n\phi_j^R)} \quad \text{(Eq. 7)}$$

where n is the atom fraction of deuterium; V_n is the observed velocity at n fraction of deuterium; V_0 is the observed velocity in water (H_2O); v_T is the number of protons transferred in the transition state; v_R is the number of protons transferred in the reactant state, and ϕ is the fractionation factor defined as Equation 8,

$$\phi = (X_i^D/X_i^H)/(n/(1 - n)) \quad \text{(Eq. 8)}$$

where X_i^D and X_i^H are the mole fractions of deuterons and protons in the ith transition or reactant state whereas the subscripts T and R refer to the transition and reactant state, respectively (45, 46). At pH 10.50, the best fit obtained exhibited a straight line (Fig. 5), suggesting the involvement of one proton in the catalytic reaction. However, at pH 6.50, the data significantly deviate from linearity, and the best fit obtained required a polynomial function, suggesting at least two protons are transferred in the transition state at this pH. Because the largest deviation for theoretical proton inventory curves occurs at atom fractions of 0.5 (47), calculation of a mid-point partial solvent isotope effect often helps in determining the number of protons involved in the catalytic reaction. The following equations, derived by Elrod *et al.* (47), allowed the calculation of mid-point partial solvent isotope effects when the experimental

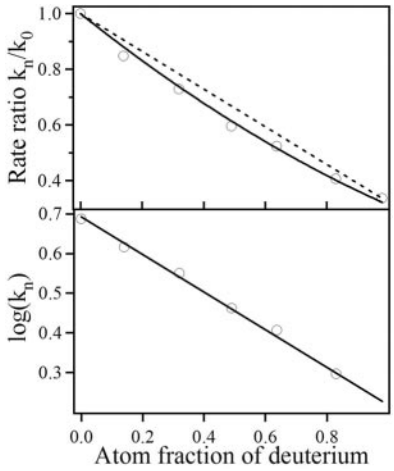

FIG. 6. **Plots of proton inventory and log(k_n) *versus* atom fraction of deuterium for E151D-AAP at pH 6.50.** *Upper panel*, the *solid line* represents a fit to Equation 8. *Lower panel*, *solid line* represents a fit to Equation 9.

data were obtained at different atom fractions. For a one-proton reaction (Equation 9),

$$V_m/V_1 = (1 - n_m)(V_0/V_1) + n_m \quad \text{(Eq. 9)}$$

whereas a two-proton reaction (equal isotope effects) can be written as Equation 10,

$$V_m/V_1 = ((1 - n_m)(V_0/V_1)^{1/2} + n_m)^2 \quad \text{(Eq. 10)}$$

and generalized solvation changes can be determined using Equation 11:

$$V_m/V_1 = (V_0/V_1)^{(1-n_m)} \quad \text{(Eq. 11)}$$

where n_m is atom fraction of deuterium with velocity V_m. The experimental and calculated mid-point partial isotope effects are presented in Table II. At pH 10.50, comparison of the theoretical and experimental mid-point partial isotope effects suggests that one proton is transferred at this pH. On the other hand, at 6.5 the mid-point partial isotope effects observed for rAAP suggest two protons are transferred, whereas general solvation changes likely dominate for E151D-AAP at this pH value. Because K_m was found to be independent of pH in the range 10.1–10.5 under the conditions used, $^{D}(k_{cat}/K_m)$ values were calculated for rAAP (1.7) and E151D-AAP (1.9).

Temperature Dependence of k_{cat} and K_m for E151D-AAP—The hydrolysis of L-*p*NA was measured in triplicate between 21 and 60 °C for E151D-AAP, and the observed k_{cat} values increased with increasing temperature. These data are very unusual because most enzymes undergo some denaturation at temperatures above 50 °C resulting in a decrease in V_{max} (48). In a simple rapid equilibrium $V_{max}/[E] = k_p$, the first order rate constant. Because the enzyme concentration was not altered over the course of the experiment, an Arrhenius plot was constructed by plotting $\ln k_{cat}$ *versus* $1/T$ (Fig. 7). A linear plot was obtained, indicating that the rate-limiting step does not change as the temperature is increased (48). From the slope of the line the activation energy, E_a, for temperatures between 291 and 333 K was calculated to be 44.5 kJ/mol, 8 kJ/mol more than that observed for WT AAP (Table III) (37). Because the slope of an Arrhenius plot is equal to $-E_{a1}/R$, where $r = 8.3145$ JK^{-1} mol^{-1}, other thermodynamic parameters were calculated by the following relations: $\Delta G^{\ddagger} = -RT\ln(k_{cat}h/k_BT)$, $\Delta H^{\ddagger} = E_a - RT$, $\Delta S^{\ddagger} = (\Delta H^{\ddagger} - \Delta G^{\ddagger})/T$, where k_B, h, and R are the Boltzmann, Planck, and gas constants, respectively (Table III).

DISCUSSION

Metalloproteases containing co-catalytic active sites are widely regarded as promising targets for drug discovery, but efficient drug discovery has been hampered by the lack of mechanistic detail for this class of enzymes. One enzyme in this class, AAP, although not a specific pharmaceutical target at this time, is one of the best mechanistically characterized co-catalytic metalloproteases; however, an important mechanistic question that has yet to be answered regarding AAP or any co-catalytic metalloprotease is as follows: What residue functions as the general acid/base during catalytic turnover? Based on x-ray crystallographic data, an active site carboxylate group, Glu-151, was implicated as the general acid/base because it forms a hydrogen bond with the bridging water/hydroxide molecule in the resting enzyme (19). Glu-151 has been proposed to assist in deprotonating the metal-bound water molecule to a more nucleophilic hydroxo moiety, similar to that of Glu-270 in carboxypeptidase A (49); however, no data have been reported to substantiate this hypothesis. In order to determine the role of Glu-151 in catalysis, we have prepared the AAP-altered enzymes where Glu-151 was changed to an aspartate, alanine, or glutamine residue.

The specific activity of E151D altered AAP was determined in the presence of L-*p*NA as the substrate. Kinetic parameters for Zn(II)-loaded WT, E151D, E151Q, and E151A AAP indicate that, in general, the effect on activity is due to a decrease in k_{cat} (Table I). Most interesting, replacement of Glu-151 with residues that are still capable of transferring a proton or forming hydrogen bonds such as aspartate or glutamine provide AAP enzymes that remain active but exhibit only 0.05 and 0.004% of the observed WT AAP activity, respectively. In both cases, the K_m values do not change indicating that substrate interacts normally with the active site. Replacement of Glu-151 with an alanine residue results in a totally inactive enzyme. These data indicate that Glu-151 is absolutely required for catalytic turnover even though it does not function as a Zn(II) ligand.

The observed molar absorptivities and absorption maxima for [Co_(E151D-AAP)] and [CoCo(E151D-AAP)] at pH 7.5 are consistent with both Co(II) ions residing in a five- or six-coordinate environment (34). Comparison of these data to those previously reported for Co(II)-substituted WT AAP suggest some structural perturbations upon substitution of Glu-151 with an aspartate. For WT AAP, the addition of one Co(II) ion at pH 7.5 provides a visible absorption spectrum with a band at 525 nm (ϵ_{525} ~50 M^{-1}cm^{-1}) (34). Addition of a 2nd eq of Co(II) increases the absorption intensity at 525 nm to ~70 M^{-1}cm^{-1}. However, the addition of more than 2 eq of Co(II) to WT AAP does not alter the intensity or position of the observed absorption band. Whereas the molar absorptivities and absorption maxima of [Co_(E151D-AAP)] and [CoCo(E151D-AAP)] are similar, the titration data are markedly different. Plots of molar absorptivity *versus* equivalents of Co(II) added to E151D-AAP allowed the number of bound metals and their corresponding K_d values to be determined. E151D-AAP was found to bind two divalent metal ions, which is identical to the WT enzyme; however, the metal binding constant for the first metal binding site decreased ~10,000-fold compared with Zn(II)-loaded WT AAP (K_d = 95 μM for Co(II) in E151D-AAP *versus* 0.052 μM for Co(II) in WT AAP) (17, 50).[3] Based on the x-ray crystal structure of WT AAP (19, 22, 43), Glu-151 forms a hydrogen bond to the water molecule that bridges between the two active site Zn(II) ions. Remarkably, the loss of this hydrogen bonding interaction does not appear to disturb the coordination number

[3] S. I. Swierczek, K. Baron, S. Mitra, and R. C. Holz, manuscript in preparation.

TABLE II
Comparison of the experimental midpoint solvent isotope effects with calculated midpoint solvent isotope effects

All experiments were carried out using L-*p*NA as the substrate. Experimental and theoretical midpoint isotope effects were calculated at 0.49 atom fraction of deuterium.

Enzyme	V_0/V_1	Midpoint solvent isotope effect V_m/V_1	Calculated midpoint solvent isotope effect		
			One proton	Two protons	Generalized solvation changes
rAAP (pH 6.5)	2.85	1.86	1.95	1.83	1.71
E151D (pH 6.5)	3.0	1.85	2.00	1.93	1.78
rAAP (pH 10.5)	2.81	1.99	1.92	1.82	1.69
E151D (pH 10.5)	2.93	1.97	1.98	1.86	1.73

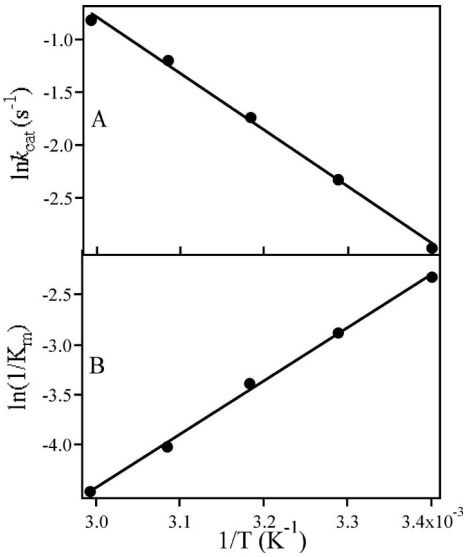

FIG. 7. *Upper panel*, Arrhenius plot for the hydrolysis of L-*p*NA by E151D-AAP. *Lower panel*, K_m *versus* temperature. The *error bars* are smaller than the markers used.

TABLE III
Thermodynamic parameters for the hydrolysis of L-pNA by WT AAP and E151D-AAP

		AAP	E151D
$E + S \rightarrow ES$	ΔG^0 (kJ/mol)	−6.1	−6.3
	ΔH^0 (kJ/mol)	−42.6	−44.4
	ΔS^0 (J/mol)	−122.5	−127.9
$ES \rightarrow (ES{\cdot\cdot}EP)^{\ddagger}$	$\Delta G^{\ddagger}$ (kJ/mol)	62.1	79.6
	$\Delta H^{\ddagger}$ (kJ/mol)	34.0	42.0
	$\Delta S^{\ddagger}$ (J/mol)	−94.2	−126.2
	E_a (kJ/mol)	36.5	44.5

of the metal ions but markedly alters the first metal binding event.

The catalytic role of Glu-151 was further examined by recording the pH dependence of the kinetic parameters k_{cat} and K_m. Based on available kinetic and x-ray crystallographic data, the simplest model was used that describes the observed changes in ionization states of active site residues with changing pH. This model (Scheme 1), which is nearly identical to that proposed by Baker and Prescott (30), assumes the following: (i) upon protonation of the substrate, its interaction with the enzyme becomes weaker, (ii) the substrate binding step leading to the formation of an enzyme-substrate complex follows steady-state kinetics (*e.g.* the enzyme, substrate, and enzyme-substrate complex are at equilibrium and k_{-1} is larger than k_2 as neither the substrate nor the product are sticky, and k_2 is the rate-limiting step (*i.e.* C—N bond breaking)); and (iii) ionizable groups on the enzyme ionize independently from each other. Each of these assumptions is consistent with the vast literature of kinetic, spectroscopic, and x-ray crystallographic studies (2). Fits of the pH dependence of K_m for both rAAP and E151D-AAP by using this model provides information regarding ionizing groups on the free enzyme, the free substrate, and in the enzyme-substrate complex (Equation 4). Inspection of a plot of logK_m *versus* pH for WT AAP reveals four inflections at 4.8, 5.3, 7.5, and 9.9. For E151D-AAP, a similar set of inflections was obtained except that the pK_a value observed at 4.8 for rAAP shifts to 4.2 in E151D-AAP. The inflection observed at 9.9 is similar to that reported by Baker and Prescott (30). These data suggest that an enzyme residue is required to be in the protonated form for the substrate to bind. The apparent pK_a value obtained suggests a tyrosine residue (pK_a of 10.5), one of which (Tyr-225) was previously implicated in hydrogen bond formation with the substrate (38, 42, 43). The pK_a value observed at pH 7.5 suggests that a protonated form of the substrate or a group on the enzyme results in decreased substrate binding affinity assisting in *E*S complex formation. This pK_a value is assigned to the deprotonation of the N-terminal amino group of L-*p*NA, which exhibits a pK_a of 7.74 (30). This assignment is also consistent with the observed pH dependence of the substrate-like competitive inhibitors *n*-valeramide and isoamyl alcohol, whose pH profiles do not exhibit an inflection point at the pH range 4–9 (30). Therefore, the protonated form of the substrate, L-*p*NA, likely binds to the enzyme less tightly than the deprotonated form.

Based on the large number of kinetic, spectroscopic, and x-ray crystallographic studies reported for AAP (2), the pK_a value observed at 4.8 in rAAP and WT AAP (30) was assigned to the deprotonation of Glu-151. Similarly, it follows that the pK_a value observed at 4.2 for E151D-AAP was assigned to the aspartate residue in position 151. This is consistent with pK_a values of free glutamate and aspartate, 4.07 and 3.90, respectively; however, the active site environment likely affects their ionization constants. Plots of logk_{cat} *versus* pH for rAAP and E151D-AAP are nearly identical and indicate that k_{cat} is constant for pH values between 7 and 10.75 (Figs. 3*B* and Fig. 4*B*). Fits of logk_{cat} *versus* pH for both rAAP and E151D-AAP provide a pK_a value of 5.2. These data indicate that one ionizable group (pK_{ES}) must be deprotonated in the *E*S complex for catalysis to occur (Scheme 1) and that a similar process is responsible for the observed changes in k_{cat} for both enzymes. The simplest explanation of the observed effect would be the assignment of this ionization constant to a carboxylic acid in the enzyme-substrate complex; however, a change in the rate-limiting step of the reaction cannot be entirely ruled out. Additional support for the assignment of this ionization constant at 5.2 to Glu-151 in the enzyme-substrate complex is provided by the temperature dependence of this pK_a. Bienvenue *et al*. (44) determined ΔH_{ion} of the group with a pK_a of 5.2, to be 25 kJ/mol, well below the value for the proposed nucleophile (46–54 kJ/mol). Thus, the observed pK_{ES} at 5.2 likely represents the ionization of a carboxylate residue that is required to be in an unprotonated form for the catalytic reaction to occur. The pK_a values for enzyme-centered ionizable groups were obtained from plots of log(k_{cat}/K_m) *versus* pH (Equation 6) (51). Fits of log(k_{cat}/K_m) *versus* pH for rAAP and E151D-AAP provide two ionizations

with pK_{a1} = 5.0 and 4.2 and pK_{a2} = 9.9 and 9.9, respectively. Ionization constants observed at 7.5 (E151D) and 7.4 (rAAP), represent pK_{HS}, which is consistent with its assignment as the ionization of the amino group of the substrate. The absence of an inflection point at 5.0 for E151D-AAP supports the assignment of this ionization constant in rAAP and WT AAP to Glu-151. Finally, the presence of an ionizing group at pH 9.9 for both rAAP and E151D-AAP is consistent with Tyr-225, as described previously.

Proton inventory studies on rAAP and E151D-AAP were also conducted in order to further understand the role of Glu-151 in catalysis and, specifically, proton transfer events. At pH 10.50, both rAAP and E151D-AAP have only one protogenic site in the transition state, because a linear dependence is observed in plots of k_{cat} *versus* atom fraction of deuterium (Fig. 5). In addition, the calculated fractionation factors are typical for transition state proton bridges, and the observed isotope effect of 2.8 and 2.9 for rAAP and E151D-AAP, respectively, is also consistent with a single proton transfer in the transition state (44). At pH 10.50 the bridging water molecule is fully ionized; therefore, a single proton is transferred but cannot come from the deprotonation of the bridging water/hydroxide moiety. Formation of a bridging hydroxide is favored by ~200 kcal/mol, as shown by theoretical calculations, which results in a more rigid environment around the metal ions (18). Therefore, the Zn(II) ions appear to be responsible for the proper positioning of the hydroxyl group, as proposed in the catalytic mechanism (2), and this hydroxyl group interacts with Glu-151. Based on these data and those presented here, Glu-151 appears to facilitate the transfer of a proton, which is likely the rate-limiting step of the reaction at pH 10.5. In E151D-AAP the shorter aspartate carbon chain results in lower rates of catalysis because a charge/proton relay network formed by water molecules would be necessary to change the rate of proton transfer and thus the overall rate of the reaction.

Proton inventory data for rAAP and E151D-AAP at pH 6.5 are significantly different from those obtained at pH 10.5. Whereas the isotope effects are similar, 2.8 *versus* 3.1 for rAAP and E151D-AAP, respectively, the midpoint solvent isotope effect suggests the involvement of more than one protogenic site in the reaction. For rAAP, the best fit was obtained using a model containing two sites with non-identical transition states exhibiting fractionation factors of 0.76 and 0.44. Analysis of the midpoint solvent isotope effect also supports the involvement of two protons in the reaction (*i.e.* proton transfer from a water molecule to Glu-151 followed by the transfer of a proton to the newly formed N-terminal amine of the leaving group). One of the fractionation factors (ϕ_{T2} = 0.44) is similar to that obtained at pH 10.50, consistent with the proposed proton transfer in the tetrahedral transition state . The first fractionation factor (ϕ_{T1} = 0.76) is characteristic of a proton-oxygen bond (neutral oxygen, 0.8–1.2) with a conventional isotope effect equal to 1 (46). It is likely that at this pH, the protonation state of Glu-151 (whose pK_a in the enzyme substrate complex is 5.3) results in the observed effect. Thus, at lower pH values Glu-151 acts as a proton shuttle (Fig. 8), as proposed previously (2). The pK_a of this residue is elevated compared with the carboxyl group of the substrate/product allowing the proton to be transferred to Glu-151 first, followed by proton transfer to the nitrogen of the newly formed N terminus. On the other hand, the calculated midpoint solvent isotope effect observed for E151D-AAP suggests that multiple proton transfers are taking place during catalysis at pH 6.5. Proper positioning of the aspartate residue in position 151 along with the fact that the carbon chain is one methylene group shorter compared with glutamate likely slows the proton

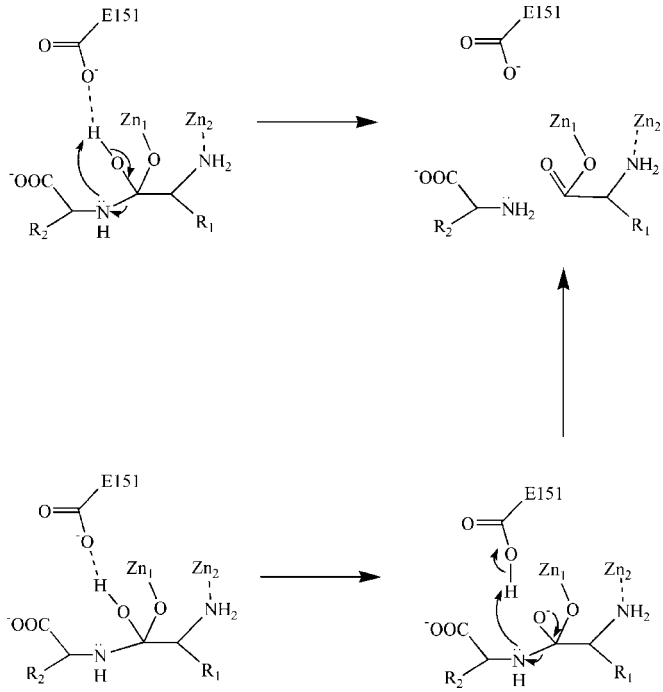

FIG. 8. **Proposed proton transfers, leading to the collapse of the tetrahedral intermediate in peptide hydrolysis by AAP.** *Arrows* indicate electron interactions/movements.

transfer step, consistent with the almost 2,000-fold decrease observed for k_{cat}. In addition, when Glu-151 is replaced with a glutamine residue, the proton cannot be transferred to the leaving group. These data are consistent with the proposed catalytic mechanism for AAP and indicate that the catalytic reaction is limited by proton transfer processes.

The temperature dependence of K_m reveals that the changes in free energy, enthalpy, and entropy for E151D-AAP are small, consistent with the pH dependence data (*i.e.* changing Glu-151 to Asp-151 does not alter the interaction of the enzyme with the substrate). Changes in the transition state , described by thermodynamic functions derived from the dependence of k_{cat} on temperature are, as expected, somewhat larger. The activation energy is 8 kJ/mol smaller for WT AAP than E151D-AAP consistent with the catalytic process occurring more slowly when Glu-151 is replaced with an aspartate. A significant change in entropy ($\Delta\Delta S^{\ddagger}$ = 32 J/mol) indicates that the interaction of the enzyme with the substrate, in the transition state, is more ordered in E151D-AAP than WT AAP. This is somewhat surprising, as the transition state should be more ordered assuming that Glu-151 is directly involved in the proton transfer step, as evident from proton inventory studies. However, there may be a higher ordering due to the formation of a water molecule network that participates in stabilizing the transition state in E151D-AAP. The latter is consistent with the proton inventory data obtained at pH 6.50, where multiple proton exchanges take place.

In conclusion, the combination of data presented here with the vast amount of kinetic, spectroscopic, and x-ray crystallographic data reported to date for AAP establishes, for the first time, that Glu-151 is absolutely required for peptide hydrolysis to occur. At pH values above 8.0, Glu-151assists in positioning the carboxyl group of the intermediate allowing direct transfer of the proton to the newly forming amine, which facilitates C–N bond breaking (Fig. 8). However, at pH values below 7.0, Glu-151 acts as a proton shuttle and abstracts a proton from the metal-bound water molecule to form a nucleophilic hydroxide moiety followed by its transfer to the newly forming N-terminal

amine (Fig. 8). Deprotonation of the metal-bound water molecule to form a nucleophilic hydroxide moiety is particularly important at pH values lower than 7.0, the postulated pK_a of the bridging water molecule, yet appears not to be the rate-limiting step based on higher stability of the μ-hydroxo bridge (18). Once the metal-bound hydroxide is formed, it can attack the activated carbonyl carbon of the peptide substrate forming a *gem*-diolate transition state complex that is stabilized by coordination of both oxygen atoms to the dizinc(II) center, consistent with the x-ray crystal structure of [ZnZn(AAP)] bound by L-leucine phosphonic acid (21). Glu-151 then provides an additional proton to the newly formed N-terminal nitrogen moiety. The product-forming C–N bond-breaking step is facilitated by proton transfer to the leaving group and is likely the rate-limiting step. This assignment is also consistent with recent thermodynamic results (37). Thus, Glu-151 is intimately involved in the reaction catalyzed by AAP and functions as both a general acid and a general base.

Acknowledgment—We thank Dr. Alvan C. Hengge for helpful discussions with regard to kinetic studies involving pH and solvent isotope effects.

REFERENCES

1. Holz, R. C., Bzymek, K., and Swierczek, S. I. (2003) *Curr. Opin. Chem. Biol.* **7,** 197–206
2. Holz, R. C. (2002) *Coord. Chem. Rev.* **232,** 5–26
3. Lowther, W. T., and Matthews, B. W. (2002) *Chem. Rev.* **102,** 4581–4607
4. Barinka, C., Rinnova, M., Sacha, P., Rojas, C., Majer, P., Slusher, B. S., and Konvalinka, J. (2002) *J. Neurochem.* **80,** 477–487
5. Boyen, A., Charlier, D., Charlier, J., Sakanyan, V., Mett, I., and Glansdorf, N. (1992) *Gene* (*Amst.*) **116,** 1–6
6. Velasco, A. M., Leguina, J. I., and Lazcano, A. (2002) *J. Mol. Evol.* **55,** 445–459
7. Barrett, A. J., Rawlings, N. D., and Woessner, J. F. (eds) (1998) *Handbook of Proteolytic Enzymes*, Academic Press, London
8. Remaut, H., Bompard-Gilles, C., Goffin, C., Frere, J.-M., and Van Beeumen, J. (2001) *Nat. Struct. Biol.* **8,** 674–678
9. Thomas, A. G., Olkowski, J. L., Vornov, J. J., and Slusher, B. S. (1999) *Brain Res.* **843,** 48–52
10. Robinson, M. B., Blakely, R. D., Couto, R., and Coyle, J. T. (1987) *J. Biol. Chem.* **262,** 14498–14506
11. Slusher, B. S., Vornov, J. J., Thomas, A. G., Hurn, P. D., Harukuni, I., Bhardwaj, A., Traystman, R. J., Robinson, M. B., Britton, P., Lu, X. C., Tortella, F. C., Wozniak, K. M., Yudkoff, M., Potter, B. M., and Jackson, P. F. (1999) *Nat. Med.* **5,** 1396–1402
12. Slusher, B. S., Thomas, A., Paul, M., Schad, C. A., and Ashby, C. R., Jr. (2001) *Synapse* **41,** 22–28
13. Witkin, J. M., Gasior, M., Schad, C., Zapata, A., Shippenberg, T., Hartman, T., and Slusher, B. S. (2002) *Neuropharmacology* **43,** 348–356
14. Tiffany, C. W., Lapidus, R. G., Merion, A., Calvin, D. C., and Slusher, B. S. (1999) *Prostate* **39,** 28–35
15. Passani, L. A., Vonsattel, J. P., Carter, R. E., and Coyle, J. T. (1997) *Mol. Chem. Neuropathol.* **31,** 97–118
16. Pulido-Cejudo, G., Conway, B., Proulx, P., Brown, R., and Izaguirre, C. A. (1997) *Antiviral Res.* **36,** 167–177
17. Prescott, J. M., and Wilkes, S. H. (1976) *Methods Enzymol.* **45,** 530–543
18. Elstner, M., Cui, Q., Munih, P., Kaxiras, E., Frauenheim, T., and Karplus, M. (2003) *J. Comput. Chem.* **24,** 565–581
19. Chevrier, B., Schalk, C., D'Orchymont, H., Rondeau, J.-M., Moras, D., and Tarnus, C. (1994) *Structure* **2,** 283–291
20. De Paola, C. C., Bennett, B., Holz, R. C., Ringe, D., and Petsko, G. A. (1999) *Biochemistry* **38,** 9048–9053
21. Stamper, C., Bennett, B., Edwards, T., Holz, R. C., Ringe, D., and Petsko, G. (2001) *Biochemistry* **40,** 7034–7046
22. Desmarais, W., Bienvenue, L. D., Bzymek, K., Holz, R. C., Petsko, A. G., and Ringe, D. (2002) *Structure* 1063–1072
23. Bennett, B., and Holz, R. C. (1997) *J. Am. Chem. Soc.* **119,** 1923–1933
24. Lipscomb, W. N., and Sträter, N. (1996) *Chem. Rev.* **96,** 2375–2433
25. Vallee, B. L., and Auld, D. S. (1990) *Biochemistry* **29,** 5647–5659
26. Vallee, B. L., and Auld, D. S. (1993) *Proc. Natl. Acad. Sci. U. S. A.* **90,** 2715–2718
27. Vallee, B. L., and Auld, D. S. (1993) *Biochemistry* 6493–6500
28. Zhang, Z.-Z., Nirasawa, S., Nakajima, Y., Yoshida, M., and Hayashi, K. (2000) *Biochem. J.* **350,** 671–676
29. Prescott, J. M., Wilkes, S. H., Wagner, F. W., and Wilson, K. J. (1971) *J. Biol. Chem.* **246,** 1756–1764
30. Baker, J. O., and Prescott, J. M. (1983) *Biochemistry* **22,** 5322–5331
31. Winzor, D. J., and Sawyer, W. H. (1995) *Quantitative Characterization of Ligand Binding*, Wiley-Liss, New York
32. D'souza, V. M., Bennett, B., Copik, A. J., and Holz, R. C. (2000) *Biochemistry* **39,** 3817–3826
33. Ustynyuk, L., Bennett, B., Edwards, T., and Holz, R. C. (1999) *Biochemistry* **38,** 11433–11439
34. Prescott, J. M., Wagner, F. W., Holmquist, B., and Vallee, B. L. (1985) *Biochemistry* **24,** 5350–5356
35. Prescott, J. M., Wagner, F. W., Holmquist, B., and Vallee, B. L. (1983) *Biochem. Biophys. Res. Commun.* **114,** 646–652
36. Bienvenue, D., Gilner, D., and Holz, R. C. (2002) *Biochemistry* **41,** 3712–3719
37. Chen, G., Edwards, T., D'souza, V. M., and Holz, R. C. (1997) *Biochemistry* **36,** 4278–4286
38. Chevrier, B., D'Orchymont, H., Schalk, C., Tarnus, C., and Moras, D. (1996) *Eur. J. Biochem.* **237,** 393–398
39. Holz, R. C., Bennett, B., Chen, G., and Ming, L.-J. (1997) *J. Am. Chem. Soc.* **120,** 6329–6335
40. Huntington, K. M., Bienvenue, D., Wei, Y., Bennett, B., Holz, R. C., and Pei, D. (1999) *Biochemistry* **38,** 15587–15596
41. Bennett, B., and Holz, R. C. (1997) *Biochemistry* **36,** 9837–9846
42. Mäkinen, K., Mäkinen, P.-L., Wilkes, S. H., Bayliss, M. E., and Prescott, J. M. (1982) *Eur. J. Biochem.* **128,** 257–265
43. Desmarais, W., Bienvenue, L. D., Bzymek, K., Holz, R. C., Petsko, A. G., and Ringe, D. (2002) *Structure* **10,** 1063–1072
44. Bienvenue, D. L., Mathew, R. S., Ringe, D., and Holz, R. C. (2002) *J. Biol. Inorg. Chem.* **7,** 129–135
45. Albery, W. J. (1975) in *Proton Transfer Reactions* (Gold, V., and Caldin, E., eds) p. 263, Chapman and Hall Ltd., London
46. Venkatasubban, K. S., and Schowen, R. L. (1984) *CRC Crit. Rev. Biochem.* **17,** 1–44
47. Elrod, J. P., Hogg, J. L., Quinn, D. M., Venkatasubban, K. S., and Schowen, R. L. (1980) *J. Am. Chem. Soc.* **102,** 3917–3922
48. Segel, I. H. (1975) in *Enzyme Kinetics: Behavior and Analysis of Rapid Equilibrium and Steady-state Enzyme Systems*, 1st Ed., pp. 847–941, John Wiley & Sons, Inc., New York
49. Christianson, D. W., and Lipscomb, W. N. (1989) *Acc. Chem. Res.* **22,** 62–69
50. Baker, J. O., and Prescott, J. M. (1985) *Biochem. Biophys. Res. Commun.* **130,** 1154–1160
51. Dixon, M., and Webb, E. C. (1979) in *Enzymes*, 3rd Ed., pp. 140–182, Academic Press

The Catalytic Role of Glutamate 151 in the Leucine Aminopeptidase from *Aeromonas proteolytica*

Krzysztof P. Bzymek and Richard C. Holz

J. Biol. Chem. 2004, 279:31018-31025.
doi: 10.1074/jbc.M404035200 originally published online May 11, 2004